THE GEOMETRIC DESIGN OF A VEHICLE BASED 3 LINE CCD CAMERA SYSTEM FOR DATA ACQUISITION OF 3D CITY MODELS

Markus Maresch, Peter Duracher
Institute for Computer Graphics
Technical University Graz
A-8010 Graz, AUSTRIA
email: {maresch,duracher}@icg.tu-graz.ac.at
www: http://www.icg.tu-graz.ac.at/~{maresch,duracher}

Commision I, Working Group 1/3

KEY WORDS: linear CCD array, facade recording, 3D city model, motion disturbance, exterior orientation.

ABSTRACT

This paper presents the geometric design of a new approach for an automatic vehicle based recording of building facades. It is based on the use of 3 partially inclined and vertical linear CCD arrays as the primary data sources. Other sensors support the retrieval of the exterior orientation. This mobile camera is used for data acquisition of the geometric model of building facades and the recording of high resolution photo texture. The requirements and constraints for this system and the theoretical background for the effect of motion disturbance due to sensor motion are discussed, and lead to the arguments for the development of the proposed system. We show recordings from a line sensor and discuss preliminary results in automatic motion detection. Methods for the creation of normalized images are explained. The major advantages of the proposed system of conventional area imaging technologies are the possibility of continuous recording, high resolution images, acceptable amount of data and the fulfilled requirements for the data acquisition of photo-realistic textured 3D city models. Our approach offers an inexpensive data acquisition method for generating photo-realistic textured city models and provides good raw data for reconstruction of a geometric model of a building's facade.

KURZFASSUNG

In diesem Bericht beschreiben wir das geometrische Design einer neuen Methode zur automatischen fahrzeugbasierten Aufnahme von Gebäudefassaden. Die Kamera basiert auf 3 teilweise vertikal orientierten CCD Zeilen als Primärsensoren, sowie weiteren Sensoren, welche die Rekonstruktion der äußeren Orientierung unterstützen. Diese mobile Kamera wird für die Datenerfassung des Geometriemodels von Gebäudefassaden und der Aufnahme von Phototextur mit hoher Auflösung verwendet. Die Anforderungen an dieses System, die Limitierung, sowie der theoretische Hintergrund für die Auswirkung von Bewegungsstörungen auf Grund der Sensorbewegung werden behandelt, und führen zu Argumenten für die Entwicklung des vorgestellten Systems. Es werden Aufnahmen mit einem Zeilensensor gezeigt und erste Ergebnisse einer automatischen Bewegungserkennung dargestellt. Methoden zur Erzeugung von Normalbildern werden erklärt. Die größten Vorteile des vorgestellten Systems gegenüber herkömmlicher flächenbasierter Aufnahmeverfahren stellen die Möglichkeit einer kontinuierlichen Aufnahme, hohe Auflösung der Zeilen und ein vertretbares Datenvolumen dar. Unser Ansatz bietet eine billige Aufnahmemethode zur Erzeugung photorealistisch texturierter Stadtmodelle und liefert gute Rohdaten für die Rekonstruktion des Geometriemodells von Gebäudefassaden.

1 INTRODUCTION

1.1 Photo-realistic textured 3D city models

Photo-realistic textured 3D city models offer new and exciting possibilities for city planning, interactive visualization of the dataset, simulation, training and effective data manipulation [GMB95].

Input-data for city models consist, among others, of 2D data from geographical information systems (GIS), digital terrain models, aerial photographs and images of facades taken from street level. The fusion of GIS data and data derived from aerial photographs results in a coarse model, the so-called building box [GMB95].

1.2 Related work

Compared to methods of [Fra95], using a camera with fish-eye lens on top of a car, [Koc93], [Koc95] using video cameras, and [AB95] using a combination of Video, GPS and odometric sensors, we propose a system based on line geometry.
The latter technology and the use of linear CCD lines in satellite scanners is described in [ORS+92], [Hof86b], [WSS94], [DLW86], [Ebn92] in great detail.

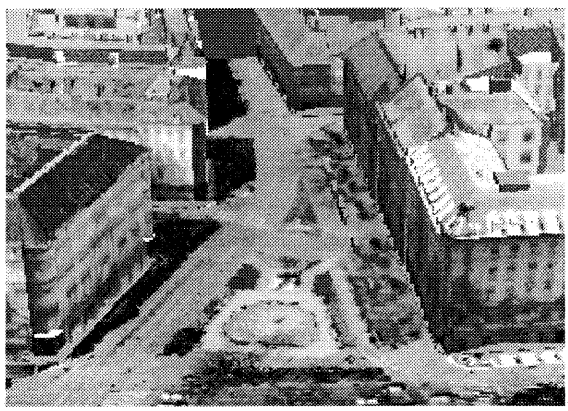

Figure 1: Snapshot of a photo-realistic textured 3D city model ("Eisenes Tor", Graz, Austria). The fusion of data derived from aerial photographs and images of facades taken from street level can be observed.

A different semi-automatic approach for building extraction and photo texture deduction from aerial images is shown in [LLS95] and other publications from the University of Bonn.

1.3 Modeling

Photo textured 3D CAD models (see figure 1) have so far been created by hand at great expense [GMB95]. Much work has to be accomplished manually [GMB95] in the generation process of a photo-realistic 3D CAD model. Transferring GIS data results in building-boxes, which are rendered with textures from aerial photography and images taken from street level. The fusion process requires extensive manual work for the modeling, thus, a high degree of detail (bay-windows, balconies,...) is only being achieved in experimental and small models.

1.4 Motivation

According to the previous discussion, the main objective of ongoing work is to find methods for semiautomatic or automated data acquisition and object reconstruction. This is valid for reconstruction from both aerial photographs and terrestrial imagery.
The support of an intelligent fusion of input data, the automatic recording of high quality photo texture of building facades and at least tools for the semiautomatic creation of geometric models of facades have to be provided.
We will focus on the design of a system for the automatic recording of building facades in this report.

2 ISSUES OF THE DATA ACQUISITION

2.1 Principal recording configuration

The principal design of the system is shown in figure 2. A vehicle based recording unit is moved laterally along a building facade. The 3 vertical CCD-lines are recording the facade continuously and simultaneously under different angles in order to allow stereo reconstruction and occlusion elimination in a subsequent processing step.

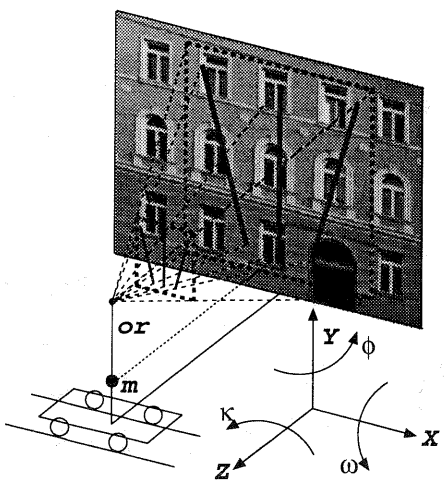

Figure 2: Principal recording configuration: The assumed coordinate system, the line sensors and the area sensor are shown. The car's center of mass is indicated by m and the vertical outrigger is denoted by or.

An additional area sensor is indicated in figure 2 to support the automatic orientation and camera tracking process. Odometric sensors and a laser distance meter support an algorithm for the reconstruction of the recording path.
For a more detailed description of the complete implementation see [Mar95b] or [MSh96].

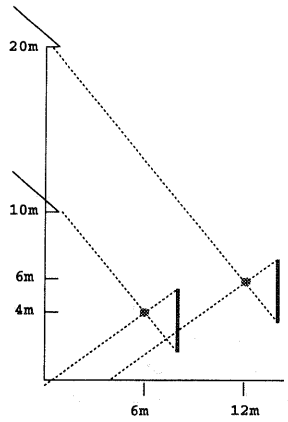

Figure 3: Recording constraints in urban environment in practice: One distance corresponds to the old part of town, and the other to the area around the center of a city with wider streets.

Two examples of recording constraints faced in urban environment are shown in figure 3. One distance corresponds to a narrow older part of a town, and the other to areas around the center of a city with wider streets.

The distance between the optical center and the facade usually is limited by the narrowness of streets and the height of the outrigger is limited by the overhead contact line of street cars and an unacceptable amount of oscillation.

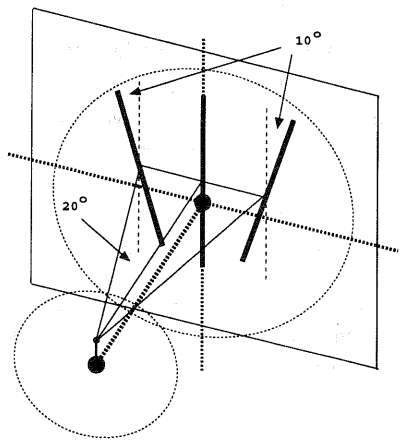

Figure 4: CCD platform: The relative orientation of 3 linear CCD arrays in one con-focal plane is shown. The shift of the center of the lines from the optical center also can be observed. The following angles were chosen: $\phi_0 \simeq 20^o$, $\kappa_0 \simeq 10^o$.

The similarity of the used technology to satellite scanners [Hof88] or aerial push broom applications is given for geometric concerns of the principal configuration. The difference though is the fact, that satellite scanners follow a quite smooth path over practically flat terrain with no regular structure, while the facade scanner has to operate along a rough path along assumed planes with the knowledge of regular vertical and horizontal edges.

The shift of the center of the linear CCD lines from the optical axis is shown in figure 4. This is done in accordance to figure 3 to omit recordings of ground regions and to keep the advantage of parallelism between object and sensor plane.

2.2 Requirements and constraints

The requirements for this portable recording system are defined by the recording constraints and by supporting hardware in practice. They are also defined by the demands for the orientation and reconstruction algorithms and the expected quality for the final data of the city models.

Color	$RGB\ 24\ bits$
Object pixel size	$(0.25cm)^2$ .. $(2cm)^2$
Stereo angle(s)	$\phi \simeq 20^o$
Vehicle speed	$0.5m/s$ .. $4m/s$
Line samples	$\geq 250/sec$
Facade height	$10m$ .. $20m$
Facade width	$100m\ min.\ at\ one\ go$
Distance to facade	$5m$ .. $12m$
Optical center	$3m$ .. $4m$
Storage recording speed	$\leq 4\ MB/sec$
Luminance	$\leq 100\ cd/m^2$

Table 1: Requirements and constraints: This table shows the design background for an experimental recording system.

Some of these constraints can not be avoided in practice. The system requirements defined in table 1 also reflect practical concerns for an inexpensive implementation.

An experimental prototype showed two more remaining problems related to linear CCD arrays:

- Sensitivity: To avoid shadows, hazy weather provides the preferred lighting conditions for recording. Unfortunately only few types of commercially available sensors allow this short exposure time at the luminance values.
- Shift rate: Sensitive sensors usually show low shift rates. Therefore many types of available linear CCD arrays must be excluded from further considerations.

The constraints explained above force a reduction in the requirements due to the necessary aim of practical, cheap implementation. Nevertheless we aim to increase the vehicle speed as soon as the effect of limiting constraints known so far becomes less important.

3 DIFFERENTIAL OBSERVATIONS

3.1 The effect of motion disturbance

Considering the principal recording configuration as indicated in figure 2 we face motion disturbance caused by the roughness of the street. The need for automatic and robust motion detection and elimination leads to investigations of the effect of motion disturbance.

We will develop the theoretical framework for the observable effect of motion disturbance first, and will then discuss the possibilities for the separation of correlated motion disturbance parameters. In the next section we will discuss the proposed algorithm for the actual motion detection.

3.2 Exterior orientation

The ideal recording path has to be provided by data from geographical information systems a priori at least to an accuracy of about 1m. Due to the motion disturbance of the vehicle we have to face a camera path different from the ideal. Each triple line sample has a different exterior orientation $(X_t, Y_t, Z_t, \omega_t, \phi_t, \kappa_t)$ for time t. Considering high sample rates of $\simeq$4ms a realistic chance for path tracking can be shown to exist, because the orientation parameters in a sequence of samples can be approximated by polynomials [KW86], [Ebn92]. Compared to the interpolation of parameters of exterior orientation [MHK94], which relies on operator selected, so-called update points, which are obviously rare, in our case **each** observation can contribute to a stable reconstruction of the camera location.

3.3 Differential observations

For the elimination of motion disturbances of the 6 parameters of the exterior orientation the geometric differential equations are discussed. Equations of table 2 from [RPgbg78], [Gru94] were modified to reflect the separation of the central mass, being the center of motion, and the optical center given by an outrigger (see also figure 2).

	dx	dy
dX_0	-1	0
dY_0	0	-1
dZ_0	$-\frac{x}{z}$	$-\frac{y}{z}$
$d\omega$	$-\frac{x*(y+or_y)}{z}$	$-z*(1+\frac{(y+or_y)^2}{z^2})$
$d\phi$	$z*(1+\frac{x^2}{z^2})$	$\frac{x*y}{z}$
$d\kappa$	$y+or_y$	$-x$

Table 2: Differential object coordinate changes caused by sensor motion, dx and dy change in general.

We assume a local coordinate system with origin at the perpendicular projection of the optical center at the facade. So coordinates x, y, z of table 2 have to be scaled by $\frac{Z_0}{c}$ and translated by vector $\overrightarrow{or_y + m_y}$ in practice.

3.4 Perpendicular vertical sensor

For vertically oriented linear CCD arrays not all motion parameters are observable, and their effect can not always be separated as there are correlated pairs of parameters.

Observing the perpendicular and vertical CCD line, only y, z and ω changes can be recognized, which is obvious in comparison to the dy-column in table 2 where the dy-value of x is always zero, and the dy-values of ϕ and κ become zero for $x = 0$.

The first improvement in increasing the observations can be achieved by changing the observation angle ϕ not to be perpendicular. This fact is reflected in table 2 for x not being zero any more ($x = \pm Z_0 * \tan(\phi)$) . But this change is mainly forced by the requirement of simultaneous recording under different angles to allow for stereo reconstruction in a later process. The information obtained by intersection of vertical lines on the object with the sensor line still is not used.

The change of orientation, although obvious and caused by other reasons, now allows to observe the effect of ϕ and κ distortions.

This implementation shows two pairs of highly correlated motion parameters: The effect of pixel shifts in y direction in image coordinates can not be separated for y and ω coordinate changes of the sensor in a robust way. The effect of change of these two parameters is similar because they are correlated. The ratio of the ω and y coordinate changes can be expressed as a function of y as follows:

$$\frac{d\omega/dy}{dY_0/dy} = Z_0 * (1 + \frac{y^2}{Z_0^2}) \qquad (1)$$

Equation (1) shows more significant changes of ω compared to y off the center of the image, but the range of the ratio remains in (Z_0 .. $2 * Z_0$) in practice. The observations of differential changes of these two parameters therefore are highly correlated and the effect is hard to distinguish.

Equivalent considerations are valid for x direction and x and ϕ change.

3.5 Inclined sensor

The most natural sensor orientation, perpendicular and vertical, has disadvantages which have to be compensated. Therefore we develop the formulae for the effect of differential motion observed by an inclined sensor as suggested in figure 4.

The idea is mainly driven by the possible observation of intersection of vertical edges on the object with the sensor line. Hofmann [Hof86a] also suggested to arrange the outer CCDs of a satellite scanner not to be parallel with the perpendicular CCD line to improve the stability in bundle adjustment. For the facade scanner this method obviously allows to observe differential changes in x-direction.

The use of κ rotated forward and backward CCDs implicates the transition to lines in the form of $dy = a * dx$ as described in [Gru94]. This leads to a compound observable change in y-direction by using the dy-column of table 2 and adding the dx-value multiplied by $(-a)$ to each term (table 2 right column).

The equations of table 3 reflect the observable differential change of object coordinates caused by sensor motion of an inclined sensor.

Arranging the 3 CCD lines as shown in figure 4 appears to combine several advantages:

- Simultaneous recording under 3 different angles,
- Maximizing the observations of differential motion,
- Added information of intersections with vertical edges.

	$\mathbf{dy - a * dx}$
dX_0	a
dY_0	-1
dZ_0	$\frac{a*x-y}{z}$
$d\omega$	$\frac{a*x*(y+or_y)}{z} - z * (1 + \frac{(y+or_y)^2}{z^2})$
$d\phi$	$-a * z * (1 + \frac{x^2}{z^2}) + \frac{x*y}{z}$
$d\kappa$	$-a * (y + or_y) - x$

Table 3: Differential object coordinate changes caused by sensor motion of an inclined sensor.

3.6 Separation of parameters

Figures 5, 6 and 7 allow a visualization of the effect of motion disturbance caused by one parameter only. The triplets are in accordance with the 3 line sensors (see figure 4).

The images have been created by modifying the perspective view of a ray-tracer to perspective and parallel projection in accordance to the present line geometry. The used model presents a simplified 3D building facade. The viewpoint was laterally moved and known distortions were added.

The existing simulation environment also allows the extension of ray-tracing a model with photo texture and adding more realistic motion disturbance. It also provides great support in the development of motion and object reconstruction algorithms.

For all images a distance of $6m$ between the optical center and the facade and realistic scale in the facade object was assumed. The distortions of all parameters were chosen as sinusoidal with the same frequency and the same effective maximum. The maximum distortion in equivalent real word scale was 10 cm for x,y and z; this is equivalent to about $17 * 10^{-3}$ radian for ω, ϕ and κ.

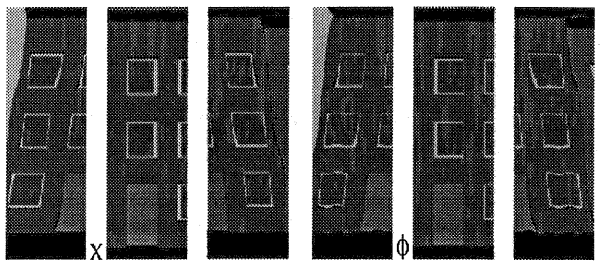

Figure 5: Simulated images with distortion for x and ϕ motion: The effect of disturbance for these 2 parameters shows different sign and is hard to separate. y disturbance, being proportional to x and y image coordinates, can only be observed under ϕ motion (see $d\phi/dy$ in table 2).

Figure 5 shows the comparison of the effect of motion disturbance of the parameters x and ϕ. While the effect is of different sign, the ratio of the effect is increasing with y,

as the image coordinate x is defined by the relative sensor orientation (see figure 4):

$$\frac{d\phi/dx}{dX_0/dx} = -Z_0 * (1 + \frac{x^2}{Z_0^2}) \quad (2)$$

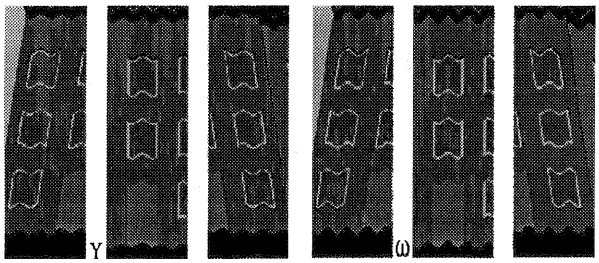

Figure 6: Distortion for y and ω motion: The effect of disturbance for these 2 parameters is also hard to separate. The observable effect for ω increases with the distance from the center of the image in y-direction (see equation (1)).

Figure 6 shows the comparison of the effect of motion disturbance of the parameters y and ω, respectively. The possible separation of these two parameters was explained while discussing equation (1).

In figure 7 the effect of a variable distance between the camera and the object and a rotation of the camera around the optical axis can be studied. Both parameters are easily separable as they are not correlated to some other parameter. We also observe the opposite effect of y-distortions in the left image for changes in z-direction, and the hardly noticeable coordinate change of κ for the perpendicular line in the center of the right triple.

Due to low resolution reproduction in this article we also present figures 5, 6 and 7 in the web [Mar95a] at a higher resolution for an interactive review.

The consequence of this consideration is the fact that a separation of these correlated pairs of parameters just mentioned still is not easy to solve. We expect to get exact information of the lateral car motion by the use of odometric sensors (see [MS96]) to solve the "x/ϕ"-pair and first experiments showed good results. The "y/ω"-pair seems to be more negligible, as y movement of the car is not so dramatic compared to rolling around the axis of forward motion when falling into road holes.

4 DATA PROCESSING

4.1 General objectives

The major objective of the geometric design of the proposed sensor is the provision of recorded data enabling subsequent algorithms to detect motion of the sensor, reconstruct the geometric model and derive photo texture. The first step therefore is the creation of a normalized image.

4.2 Characteristic of motion disturbance

The amount of motion disturbance faced by a standard mid-class car passing the front a building has to be considered.

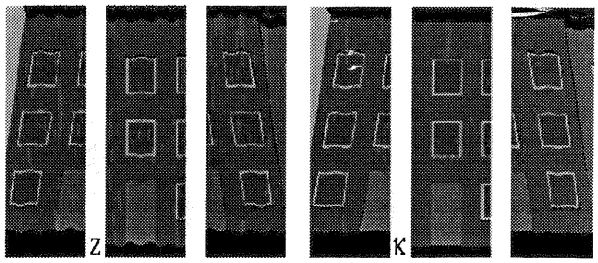

Figure 7: Distortion for z and κ motion: Both parameters are not correlated to others and therefore easily separable. The z motion results in opposite effects in y-direction; The effect of κ motion is hardly noticeable in the center line of the right triple.

First experiments showed low frequency oscillations with maximal effects of $\pm 10cm$ in object space. A detailed description of experimental recordings can be found in [MS96] or [MSh96].

4.3 A two step motion detection and elimination

We do not expect to solve the orientation process in one step. Figure 8 shows the effect of motion disturbance at $(1cm)^2$ object pixel size based on a simulation. Obviously this distortion can not be expected to be eliminated using standard image processing techniques.

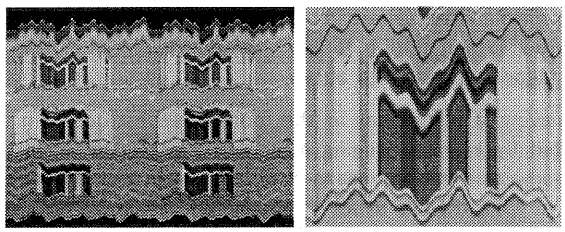

Figure 8: Simulated effect of motion disturbance of a scanned building facade.

Figure 9 shows the effect of motion disturbance on a line recording in a real environment. More details can be reviewed in [MS96].

The basic idea for the primary motion reconstruction is to add a CCD area sensor of low resolution. A series of these images together with possible match partners are shown in figure 10.

The area images have an average overlap of more than 96% in practice. The length of the observed square in object space has approximately the height of two levels of the building, which in most cases guarantees the observation of at least four windows.

A detailed description of a robust and automatic motion detection algorithm based on standard matching and affine transform can be found in [Mar96a] or [Mar96b].

The result is a precise method for automatic and robust dif-

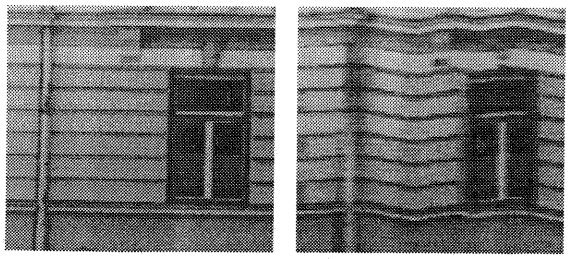

Figure 9: Comparison of a conventional area image with a line image under motion distortions (real recordings).

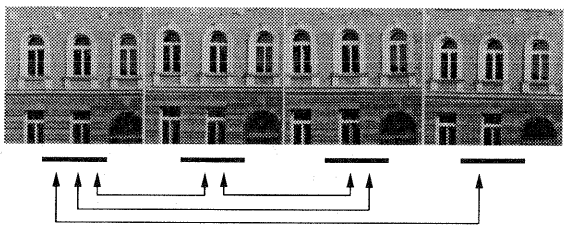

Figure 10: Motion distorted sequence of area facade samples with match partners for motion detection.

ferential motion detection and camera tracking, respectively.

In a second step we propose a re-sampling of the recorded lines onto a virtual plane. This projection is determined by the recorded lateral motion data and the reconstructed motion via the algorithm explained above.

Achieving a refinement in the motion reconstruction is expected by a line matching algorithm. The latter compares two adjacent lines by means of differences in the vertical gradient. One models small shifts and scale changes between lines using horizontal edges in the object. This is expected to lead to the final motion reconstruction.

5 CONCLUSIONS AND FURTHER WORK

This paper presents the geometric design of a CCD line based system for the recording of building facades for a more efficient way of creating photo realistic 3D city models.

The advantages of the proposed design are the continuous and simultaneous recording under different angles for stereo reconstruction and obstacle elimination, and the high quality texture recorded at an acceptable amount of data.

An introduction for the need of 3D city models and therefore the motivation for the proposed vehicle based system, the principal recording, requirements, and the motion disturbance are discussed in detail.

Research and results in the first step of elimination of motion disturbance was shown and the outline of further algorithms was introduced.

The application of the proposed system is expected to lead to a faster and better acquisition of the 3D geometry and photo-texture of 3D city models.

6 ACKNOWLEDGMENT

We express our gratitude for the support of the Austrian National Bank - Jubiläumfonds "System zur Erfassung und Optimierung digitaler Präzisionsbilder, Nr. 4871" and "System zur Erfassung und Rekonstruktion von Gebäudefassaden, Nr. 5821".

References

[AB95] T. Aussems and M. Braess. *Mobile Mapping Using a Surveying Vehicle Integrating GPS, Wheel Sensors and Digital Video Camera.* 2^{nd} Course in Digital Photogrametry, 11/1995.

[DLW86] A. Drescher, M. Lehner, and J. Wu. A common approach to navigation and geometric image correction for the stereoscopic linescan camera. In *Progress in Imaging Sensors*, 1986.

[Ebn92] H. Ebner. A simulation study on point determination for the MOMS-02/D2 space project using an extended functional model. In *ISPRS Proc., Commission IV*, pages 458–464, 1992.

[Fra95] Frank Data. Desktop surveying: First experiencies with cyclomedia. *Geomatics Info Magazine*, pages 46–51, 3/1995.

[GMB95] M. Gruber, S. Meissl, and R. Böhm. Das dreidimensionale digitale Stadtmodell Wien, Erfahrungen aus einer Vorstudie. *Vermessung und Geoinformation 83,1+2*, pages 29–36, 1995.

[Gru94] M. Gruber. Geometrische Überlegungen zum Reseauscanner. Description of differential equations and transition to line geometry, Internal Memo, Technical University Graz, 1994.

[Hof86a] O. Hofmann. The stereo-push-broom scanner DPS and its accuracy. In *Progress in Imaging Sensors*, Proc. ISPRS Symposium, pages 257–264, November 1986.

[Hof86b] O. Hofmann. Dynamische Photogrammetrie. *Bildmessung und Luftbildwesen*, pages 105–121, 3/1986.

[Hof88] O. Hofmann. A digital three line stereo scanner system. In *Internatinal Archives, Commission II*, volume 27, pages 206–213, 1988.

[Koc93] R. Koch. Automatic reconstruction of buildings from stereoscopic image sequences. *Eurographics 93*, pages 339–350, 3/1993.

[Koc95] R. Koch. 3-D Surface Reconstruction from Stereoscopic Image Sequences, 1995.

[KW86] G. Konecny and J. Wu. Analytische Streifen-Aerotriangulation für Stereo - Dreilinienabtaster. *Bildmessung und Luftbildmessung*, Heft 5(54):179–194, 1986.

[LLS95] F. Lang, T. Löcherbach, and W. Schickler. A one-eye Stereo System for Semi-Automatic 3D-Building Extraction. *Geomatics Info Magazine*, 6/1995.

[Mar95a] M. Maresch. Introduction of a CCD line camera system for recording building facades. http:// www.icg.tu-graz.ac.at/ ~maresch/ ccd.html, November 1995.

[Mar95b] M. Maresch. Kopernikusgasse, the first facade recordings using a vehicle carried camera system. http://www.icg.tu-graz.ac.at/~maresch/kop.html, November 1995.

[Mar96a] M. Maresch. Automatic camera tracking using image sequences of house facades. *submitted to ICPR 96*, 1996.

[Mar96b] M. Maresch. Submitted ICPR 96: Automatic camera tracking using image sequences of house facades. http://www.icg.tu-graz.ac.at/~maresch/pub.html, January 1996.

[MHK94] F. Müller, O. Hofmann, and A. Kaltenecker. Digital Photogrammetric Assembly (DPA) point determination using airborne three-line camera imagery - practical results. In *ISPRS Proc., Commission III, WG 1*, 1994.

[MS96] M. Maresch and D. Scheiblhofer. A vehicle based multi sensor platform for facade recording. *Accepted for ÖAGM 96*, 1996.

[MSh96] M. Maresch and D. Scheiblhofer. Accepted for ÖAGM 96: A vehicle based multi-sensor platform for facade recording. http://www.icg.tu-graz.ac.at/~maresch/pub.html, February 1996.

[ORS+92] D. Örtel, R. Reulke, R. Sandau, M. Scheele, and T. Terzibaschian. A flexible digital wide-angle optoelectronical stereo scanner. In *ISPRS Proceedings*, 1992.

[RPgbg78] Rüger, Pietschner, and Re gensbur ger. *Photogrammetrie, Verfahren und Geräte*, chapter 7, pages 243–247. VEB Verlag für Bauwesen, Berlin, 1978.

[WSS94] Y. Wang, E. Siebe, and J. Schiewe. Gereration of epipolar images from MOMS-02 linear scanner images. In *ISPRS Proceedings, Commission III, WG 2*, 1994.